EXPERIMENTAL PROGRAM AND SIMPLIFIED NONLINEAR DESIGN EXPRESSION FOR GLASS CURTAIN WALLS WITH LOW-LEVEL BLAST RESISTANCE

BENJAMIN T. KENNEDY[1], DAVID C. WEGGEL[1] & R. G. KEANINI[2]
[1]Department of Civil and Environmental Engineering,
The University of North Carolina at Charlotte, NC, USA.
[2]Department of Mechanical Engineering and Engineering Science,
The University of North Carolina at Charlotte, NC, USA.

ABSTRACT

A series of five full-scale, nearly conventional, curtain wall specimens was tested in the UNC Charlotte Structures Laboratory. Specimens were subjected to quasi-static, uniform, out-of-plane loading to failure under displacement control. The tests were performed to obtain complete resistance curves, including the nonlinear behavior of the specimens up to 'ultimate failure'. Ultimate failure was defined as mullion fracture or significant breach of the curtain wall system when viewed as the protective barrier between building occupants and the external blast load. Representative load-deflection and load-strain resistance curves are presented. The energy absorbed by the curtain wall system up to three different limit states – first cracking of glass, first yield of mullions, and fracture/breach of the system (ultimate failure) – and maximum mullion end rotations are computed from the experimental results. Ultimate energy absorption capacity – the recoverable linear strain energy plus the nonlinear energy due to formation of damage mechanisms – and maximum mullion end rotations are essential for reliable and economical design of blast resistant curtain walls. To this end, a simplified methodology is presented for analytically approximating curtain wall resistance functions that can be input to an energy expression that models nonlinear structural dynamic behavior due to an 'impulsive' loading. The blast resistance of a curtain wall can then be approximated using this procedure. It is shown that a nearly conventional curtain wall, a conventional system with two modifications – use of laminated glass lites that are structurally glazed (wet-glazed) to a conventional framing system with structural silicone sealant – had nearly 14 times the ultimate energy absorption capacity and nearly four times the blast resistance as the fully conventional system.

Keywords: Glass curtain wall; blast resistance; nonlinear SDOF design expression; static destructive tests.

1 INTRODUCTION

Economical design of curtain walls to resist extreme out-of-plane loads, such as blast loads, implies that the curtain wall can suffer significant damage in a blast event. However, in order to be a protective barrier between building occupants and the external threat, the curtain wall system must remain largely intact to prevent it from becoming a flying debris hazard and limit blast overpressures intruding into the protected space. Modeling curtain wall systems after the onset of glass cracking or mullion yielding is a significant challenge, requiring consideration of nonlinear material behavior and often nonlinear geometry. Further, the complex structural behavior of the curtain wall's individual components and their connections must be well understood.

This present work continues a long-term study in which a calibrated, elastic, finite element (FE) curtain wall model was developed [1,2]. The model is capable of simulating static and dynamic responses (before cracking or yielding of system components) under general loading and considers linear and nonlinear geometry. The FE model is presently being extended to the post-elastic regime, where the test results of full-scale curtain walls subjected to extreme out-of-plane loading, reported here, will be used in its calibration.

However, in this paper, these test results will be utilized to support the development of an approximate analytical curtain wall resistance function that can be input to a simple energy expression that models the nonlinear structural dynamic behavior of a curtain wall subjected to 'impulsive' loading, in this case a uniform blast load with a duration less than 1/5th the fundamental period of the curtain wall system [3]. The blast resistance of a curtain wall can then be approximated using this procedure. The curtain walls considered in this program will provide a low level of blast resistance and would be appropriate for scenarios where small blast threats or collateral blast damage (in the impulse-dominated regime) are of concern.

The components of glass curtain wall systems have been extensively studied. Based on the probabilistic failure prediction model for glass plates developed by Beason and Morgan [4] and the work of Vallabhan [5], ASTM E1300-09a [6] provides a design procedure for rectangular glass lites supported on one, two, three, or four edges and subjected to 3-second wind loads. Monolithic and laminated glass lites subjected to blast and impact loads, for example, have received significant attention [7–12, 33] and design charts equating blast loading to 3-second duration wind loads have been developed [13], ASTM F2248-09 [14]. Research has also been conducted on the composite action of mullions [15], and the properties of gaskets [16] and silicones [17–19] used to connect glass lites to supporting mullions.

Limited work has been reported on the overall response of curtain walls as complete systems. For example, the response of curtain walls subjected to racking as resulting from seismic shaking has been investigated [20–23]. FE modeling of system response to out-of-plane wind loading has been carried out by Craig and Goodno [24], Goodno [16], and Goodno and Craig [25]. Clift [26] provides three case studies that compare curtain walls designed for high winds to blast requirements, concluding that a design for high winds inherently provides a small amount of blast resistance. The FE models developed by Weggel *et al.* [2] were used to study the interaction between individual curtain wall components, emphasizing stresses in glass lites when the system is subjected to low level blast loads [1].

Even less research has been reported on the nonlinear response of curtain wall systems subjected to extreme out-of-plane loading. Dawson and Smilowitz [27] describe analytical procedures for the post-elastic design of blast resistant curtain walls. The authors assert that accurate nonlinear dynamic modeling requires knowledge of the phasing of the different responses of the glass and the mullions as well as accounting of the energy dissipated through inelastic deformation. They also state that current design guidelines regarding maximum useable mullion end rotations (currently 2 degrees) and corresponding mid-height deflections (L/60) are too conservative. The U.S. General Services Administration (GSA) [28] provides a testing method for glazing and window systems subjected to blast overpressures. This protocol provides definitions, sets Window Glazing Analysis Response and Design (WINGARD) as the standard for analysis and design of windows subjected to blast loads, and provides the basic reporting requirements for blast testing. ARA has recently developed a prototype tool for the GSA, WINGARD-MP, for the analysis and design of curtain wall systems subject to blast loads. This code couples WINGARD-PE, for glazing response analysis/design, with a FE analysis code to also 'determine the response of the frames and mullions in a complex multi-paned window system' [29]. However, this code is only available for GSA use.

Cussen and Van Eepoel [30] examine recent advances in analytical tools used to predict the behavior of windows and curtain walls subjected to blast loadings. They describe

the advantages and disadvantages of using single degree of freedom (SDOF) methods versus advanced analytical approaches and, through a case study, compare the resulting designs using each procedure. The SDOF method was found to be significantly more conservative for the case they presented. Edel and Kumar [31] compare three modeling techniques for a curtain wall system attached to pretensioned cables subjected to an impulsive load. The techniques include two separate single-degree-of-freedom models, including a WINGARD model, and a three-dimensional FE model. The results among the three analyses are shown to compare well during the early stages of response, but after 150 msec, where the behavior is increasingly nonlinear, the FE analyses predict larger responses.

Experimental work and additional supporting analytical work is thus needed to address the uncertainties and limited understanding associated with the post-elastic performance of curtain wall systems under extreme out-of-plane loading. As defined in this paper, a conventional curtain wall is comprised of monolithic glass lites that are dry-glazed to a conventional framing system (extruded aluminum mullions) and connected to the structural back-up with conventional anchorage devices. This type of curtain wall system, where wind is typically the governing design lateral load (pressure), makes up the majority of those in service. A nearly conventional curtain wall is defined in this paper as a conventional curtain wall with two modifications – use of laminated glass lites that are structurally glazed (wet-glazed) to a conventional framing system with structural silicone sealant – to enhance performance to extreme out-of-plane loading. The present study focuses on the elastic and post-elastic (strongly nonlinear) behavior of a family of nearly conventional curtain wall systems subjected to controlled displacement, quasi-static, uniform, out-of-plane loading. The investigation has several objectives.

First, the nonlinear behavior and failure resistance of the nearly conventional curtain walls are experimentally characterized. Two variants of the nearly conventional systems are examined: one has annealed laminated glass lites that are dry-glazed to the framing system and the other has annealed laminated glass lites that are wet-glazed to the framing system. The dry-glazed specimen used conventional compression gaskets to connect glass lites to the framing system, while the wet-glazed specimens used structural silicone sealant. Laminated glass, once cracked, gives the lites a structurally advantageous membrane-like quality, while structural silicone sealant inhibits lite-mullion detachment under load.

Second, a straight forward experimental method for estimating global curtain wall energy absorption throughout the linear and nonlinear load-deflection regimes is described. The method requires a global, i.e. area averaged, load-deflection resistance curve, which in turn requires a limited amount of spatially discrete, load-dependent deflection data.

Third, a simple semi-empirical, energy based modeling approach is proposed which allows use of curtain wall deflection data, obtained under slow (i.e. non-impulsive) loading conditions, for the prediction of curtain wall blast resistance. The proposed method thus suggests a simple route for connecting relatively inexpensive quasi-static load-deflection test results with (conservative) estimates of the curtain wall's failure resistance under blast loading.

Fourth, procedures for mapping the complex nonlinear load-response of multi-degree-of-freedom curtain wall systems to equivalent single-degree-of-freedom, nonlinear spring models, are described in detail.

Fifth, the blast resistance of three curtain wall systems – a conventional system using monolithic glass lites, a dry-glazed system using laminated glass lites, and a wet-glazed

system using laminated glass lites – are determined and compared, both with one another and with that predicted by the simple energy based model described in objective 3. While only the wet-glazed curtain wall system using laminated glass lites is recommended for low level blast applications, comparisons among the three systems are made to show how incremental improvements yield enhanced blast resistance.

In overview, this study seeks to demonstrate how relatively straight forward quasi-static test results can be combined with simple nonlinear energy based (equivalent spring) models to approximate curtain wall blast resistance that is suitable for initial design or rough analysis.

2 EXPERIMENTAL PROGRAM

2.1 Curtain wall specimens

The elevation of all curtain wall specimens is shown in Fig. 1. Specimens were nominally 3.66 m (12 ft) tall, spanning floor-to-floor, and 2.44 m (8 ft) wide. The metal framing system was Kawneer's conventional, 153 mm (6 in) deep aluminum extrusions comprised of three split screw spline vertical mullions and six tubular screw spline horizontal mullions. Four nominal 1.22 m by 1.83 m (4 ft by 6 ft) laminated glass lites were attached to the aluminum extrusions. All glass lites had a total nominal thickness of 11.11 mm (7/16 in) and were comprised of a 4.76 mm (3/16 in) annealed lite, a 1.52 mm (0.06 in) Solutia 060 polyvinyl butyral (PVB) interlayer, and another 4.76 mm (3/16 in) annealed lite; the actual thickness of the laminated glass layup was 11.05 mm (0.435 in) including the PVB interlayer. Four specimens were wet-glazed (SPS series); that is, the laminated glass lites were connected to the mullions with a 12.7 mm by 6.4 mm (0.5 in by 0.25 in)
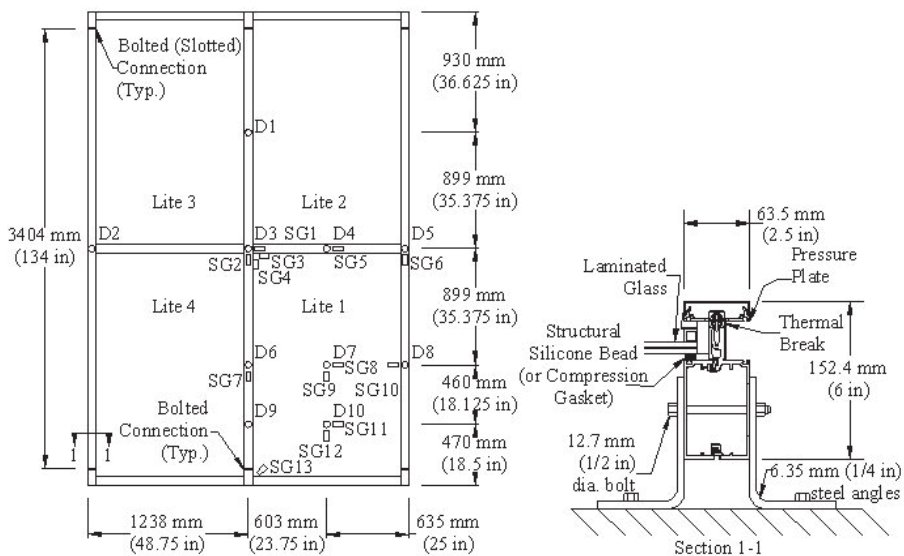

Figure 1: Elevation and section of a curtain wall specimen with instrumentation layout (inside looking out).

GE SilPruf SCS 2000 structural silicone sealant bead. One specimen was dry-glazed (SPG-1); the laminated glass lites were connected to the mullions with conventional compression gaskets. For all specimens, horizontal mullions were connected to the vertical mullions with four 25.4 mm (1 in) long screws. Each screw went through a predrilled hole in the vertical mullion and self-tapped into a receiving screw spline in the horizontal mullion. Each end of the three continuous vertical mullions was connected to the reaction frame with one 12.7 mm (1/2 in) diameter bolt that passed through double steel angles. The bottom connections had 1.59 mm (1/16 in) oversized holes (simulating a pin), and the top connections had 1.59 mm (1/16 in) oversized slots to allow for small vertical in-plane movements (simulating a roller). This effectively connected the top and bottom of each vertical mullion to the structural backup as it would be in the field (See Section 1-1 in Fig. 1). Curtain wall specimens were also supported along their outer vertical edges with rollers that prevented horizontal in-plane deflections but allowed out-of-plane deflections. This was designed into the experimental set-up to simulate the in-plane stiffness that would be provided by adjacent curtain wall panels.

Modern curtain walls typically have a monolithic outboard glass lite in addition to an inboard glass lite separated by a sealed air space to make up an insulating glazing (IG) unit. These units, if properly designed, have superior thermal properties and condensation resistance than a single glass lite. In this program the outboard lite was not included for safety concerns and other practical purposes during the testing phase. Therefore, the specimens described in this paper do not have the small additional energy absorption capacity that the outboard lite would provide.

2.2 Instrumentation

All test specimens were instrumented with 13 strain gages (SG1–SG13) and 10 wire potentiometers (D1-D10) to measure deflection; see Fig. 1. Instrumentation was concentrated on the lower right lite, Lite 1 (when viewed from inside looking out), since the curtain wall possessed two-fold symmetry. Wire pots D1 and D2 were used to check deflection symmetry about the horizontal and vertical axes of symmetry, respectively.

2.3 Aluminum mullions

Coupons were cut from horizontal and vertical mullions and tested in tension to obtain stress-strain curves for the 6063-T6 aluminum. The procedure described in ASTM B557 [32] was used to obtain the material constants given in Table 1.

The yield and ultimate strengths from coupon testing were found to be 29% and 20% higher than the commonly specified *minimum* values of 172 MPa (25000 psi) and 207 MPa

Table 1: 6063-T6 aluminum material constants.

Constant	Value
Yield Strength (F_y)	241 MPa (35000 psi)
Ultimate Strength (F_u)	259 MPa (37500 psi)
Young's Modulus (E)	61.4 GPa (8.9×10^6 psi)

Table 2: Vertical mullion section properties.

Property	Value
Area (A)	1.757×10^3 mm^2 (2.72 in^2)
Centroid* ($\bar{y}$)	80.77 mm (3.18 in)
Moment of Inertia (I)	2.602×10^6 mm^4 (6.25 in^4)
Plastic Section Modulus (Z)	4.930×10^4 mm^3 (3.01 in^3)

*Relative to bottom (tensile) extreme fiber.

(30000 psi), respectively. However, Young's modulus was found to be 11% lower than the typically referenced value of 68.9 GPa (10×10^6 psi). Part of the discrepancy is due to the fact that the tensile modulus is approximately 2% less than the compression modulus.

Table 2 provides the section properties of the vertical mullions. Values for the area and centroid were computed solely from scaled section drawings using AutoCAD. The effective moment of inertia, however, was determined experimentally from simply supported specimens subjected to three-point loading. Two tests were conducted and the averaged result is given in Table 2. The effective moment of inertia was found to be 70% of the full composite moment of inertia computed from scaled section drawings using AutoCAD; the AutoCAD-computed composite moment of inertia included the male and female mullion halves and the pressure plate as shown in Section 1-1 of Fig. 1. More importantly, results from the mullion bending tests at high loads indicated an effective plastic section modulus that was 76% of the full composite plastic section modulus computed from scaled section drawings using AutoCAD.

2.4 Laminated glass lites

Tests on laminated glass lites were not conducted in this experimental program. Instead, the maximum load resistance of 3.67 kPa (76.7 psf) was estimated using the procedure of ASTM E1300-09a [6]; this resistance is based on a 0.008 probability of breakage (cracking) of the lite and a 3-second load duration. Using the glass failure prediction model presented in Beason and Morgan [4] to adjust for a probability of breakage of approximately 0.500 (the lite's median resistance value), the lateral resistance becomes approximately 7.86 kPa (164 psf). Finally, adjusting from the 3-second load duration to the expected 30-minute load duration of the destructive panel tests, the lateral resistance becomes 5.27 kPa (110 psf).

2.5 Structural silicone sealant

For these material strength tests, the specimens consisted of a short segment of mullion with an aluminum tab (simulating the glass) attached to it with a 50.8 mm (2 in) long bead of structural silicone sealant; the bead's cross section was 12.7 mm by 6.4 mm (0.5 in by 0.25 in). The bead was loaded in tension after the tab was rotated 30 degrees relative to the plane that would be occupied by an uncracked glass lite. This was done to simulate the stress field in the bead once the glass lite cracked and transitioned from plate bending to membrane action; this is more representative of the state of stress the sealant bead would experience

when it was most critically loaded. The average ultimate load resisted by the bead in this condition was 9.81 N/mm (56 lb/in).

2.6 Free vibration tests

Prior to the destructive tests, three free vibration tests were conducted on specimen SPS-1 to determine the natural frequencies of the elastic curtain wall system. Support conditions were identical to those used in the destructive tests; however, for these tests four accelerometers were connected to the curtain wall at locations D2, D3, D5, and D7 as shown in Fig. 1. The middle vertical mullion of the curtain wall was given an initial horizontal displacement of approximately 12.7 mm (0.5 in) at its mid-height and zero initial velocity. The tests were initiated by tripping a quick-release mechanism and allowing the specimen to freely vibrate. After Fourier processing the acceleration time series data, the fundamental natural frequency of the curtain wall system was found to be 67.2 rad/s.

2.7 Destructive tests

For each of the destructive tests a uniform load was applied to the exterior face of the curtain wall using the specially designed airbag loading apparatus shown in Fig. 2. The butt of the hydraulic loading jack was connected to the reaction frame, and the piston pushed the rolling load frame which held four airbag pans that were free to rotate about their horizontal centers. Each of the four pans pushed individual but identical airbags against the curtain wall specimen, distributing the resultant force (measured by the load cell) to a uniform pressure applied over the entire curtain wall specimen. The tests were conducted under displacement control with a linear ramp of 12.7 mm/min (0.5 in/min) so that the descending branches of the curtain wall resistance curves could be obtained.

Figure 3 shows curtain wall specimen SPS-2 before loading and during loading just after the center vertical mullion fractured. All wet-glazed specimens were loaded until the center vertical mullion fractured; however, the curves presented in this paper are only plotted up to 'ultimate failure' as defined below.
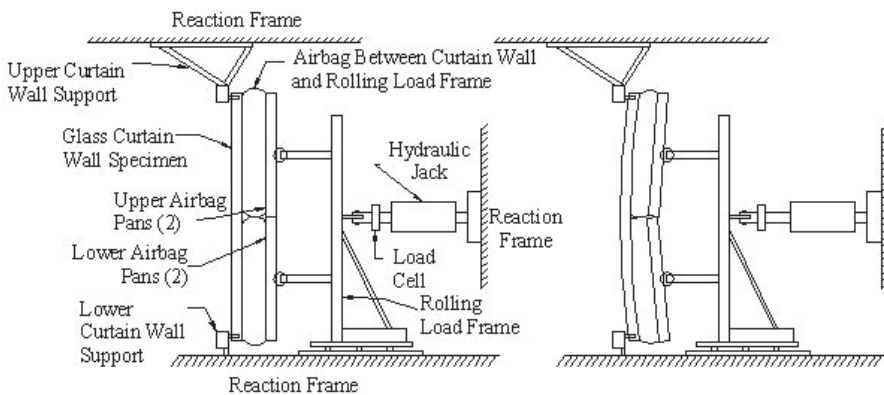

Figure 2: Side elevation of curtain wall specimen, loading apparatus, and reaction frame: unloaded specimen (left) and loaded specimen (right).
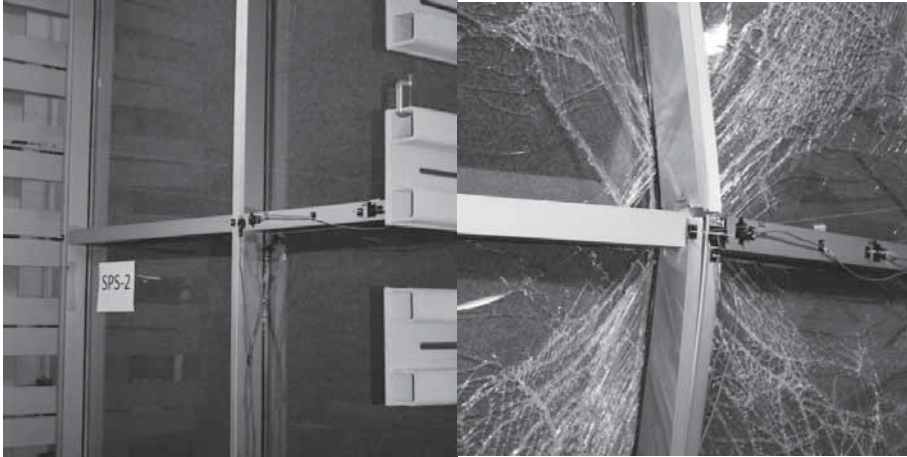
Figure 3: Curtain wall specimen SPS-2 in the reaction frame (inside looking out): unloaded specimen (left), loaded specimen just after mullion fracture (right).

2.8 Ultimate failure definition

A properly designed curtain wall can be an effective protective barrier between the external extreme load (i.e. blast overpressures) and the building occupants. In this study 'ultimate failure' was considered to be a significant breach of that 'barrier'. Specifically, ultimate failure was attained if one of the following three events occurred:

1.   fracture of an aluminum mullion (Failure Type 1),
2.   bolted or screwed connection failure (Failure Type 2), or
3.   separation of glass lites from supporting mullions (tearing of structural silicone sealant) for a continuous length of 610 mm (24 in) (Failure Type 3).

For the dry-glazed specimen (using conventional compression gaskets), Failure Type 3 required a slightly different interpretation; when 610 mm (24 in) of a glass lite's edge pulled out of the glazing pocket by nearly 12.7 mm (0.5 in), the length of the lite's bite, a separation failure occurred.

3 RESULTS

3.1 Resistance curves

Experimentally determined resistance curves can provide insight into the nonlinear behavior of the curtain wall system. 'Local resistance curves' emphasize the behavior of the curtain wall at the location of an individual sensor. For example, Fig. 4 shows a representative curve (from specimen SPS-2) for resultant force resistance versus mid-height deflection of the center vertical mullion. Each sudden drop in resistance occurs when a different glass lite breaks and transitions from plate bending behavior to membrane behavior, but the sequence of glass lite breakage cannot be determined from this curve alone.
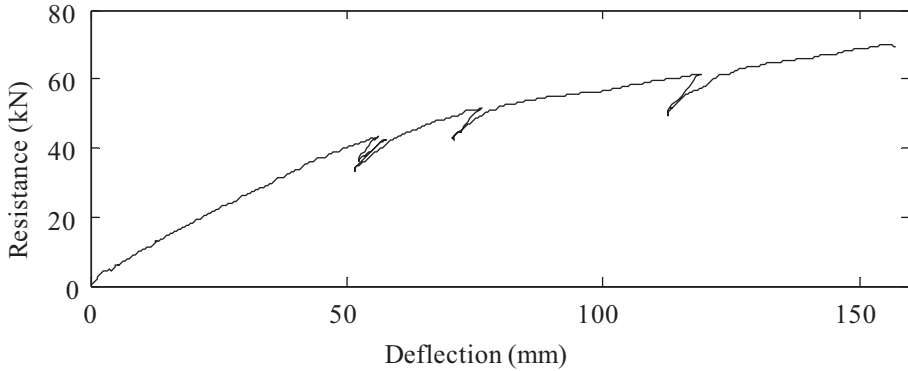
Figure 4: Resultant force resistance versus D3 deflection (local resistance curve).
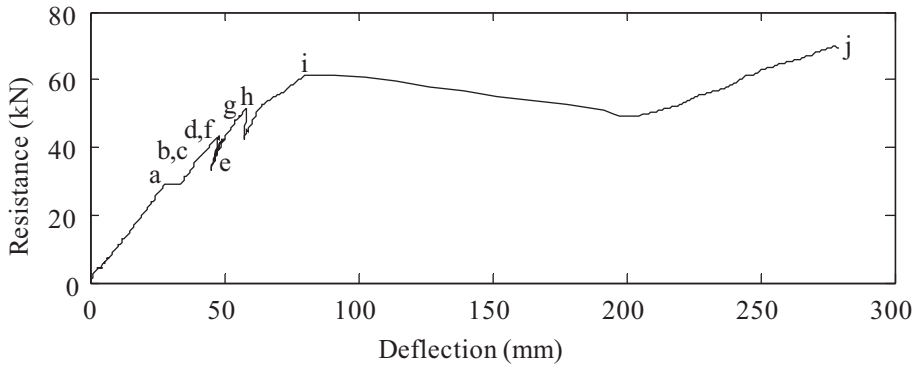

Figure 5: Resultant force resistance versus D7 deflection (local resistance curve).

Figure 5 is a representative curve for resultant force resistance versus D7 deflection (deflection at the center of Lite 1). The significant events for this test are labeled in the figure and are briefly described as follows:

a. first cracking of Lite 1, with some portion of plate bending behavior remaining;
b. first cracking of Lite 3, with some portion of plate bending behavior remaining;
c. first cracking of Lite 4, with some portion of plate bending behavior remaining;
d. additional cracking of Lite 3, leading to membrane behavior of the lite;
e. first cracking of Lite 2, with some portion of plate bending behavior remaining;
f. additional cracking of Lite 2, leading to membrane behavior of the lite;
g. strain at mid-height of the center vertical mullion indicates yield;
h. additional cracking of Lite 4, leading to membrane behavior of the lite;
i. additional cracking of Lite 1, leading to membrane behavior of the lite;
j. ultimate failure: 610 mm (24 in) of continuous separation of Lite 4 from the outside vertical mullion.

The lateral resistance of the glass lites (predicted using ASTM E 1300) can be converted to a resultant force acting over the entire curtain wall (5.27 kPa × 2.44 m × 3.66 m = 47 kN). It is

interesting to note that the 47 kN resultant force appears to be the approximate 'median' resistance of the glass lites breaking in the curtain wall panel as shown in the resistance curve of Fig. 5.

Figure 6 shows the resultant force resistance versus SG2 strain, where the strain is measured at mid-height of the center vertical mullion. This plot was used to determine when the center vertical mullion yields as compared to the aluminum coupon tests.

In order to obtain a global resistance curve that represents overall curtain wall system behavior in one plot, all local force-deflection resistance curve data were substituted into interpolation functions to produce the resistance curve for a quadrant of the curtain wall. The interpolation functions estimated deflections between sensor locations (wire pots) to produce a numerical deflection function for the curtain wall system as a function of *X-Y* coordinate axes.

Figure 7 shows the coordinates and locations of the nodes used for computation of the deflection function. With the exception of node 2, each node location coincides with a sensor location or a support. Nodes 1 and 3 are at mullion supports, nodes 4, 5, 6, 7, 8, and 9 are, respectively, at the locations of D6, D7, D8, D3, D4, and D5 wire pots (compare Figs. 1 and 7). Since it is between two vertical mullion supports and is near a relatively stiff horizontal mullion that receives little load, node 2 is assumed to have zero deflection. The deflection function is given by eqn (1) and the nine individual interpolation functions are shown in Table 3.

$$\Delta(x,y) = \sum N_i \Delta_i \tag{1}$$

where N_i are the assumed interpolation functions given in Table 3, Δ_i are the measured (or assumed) deflections at each location *i* (see Fig. 7), and $x_1 = 610$ mm (24 in), $x_2 = 1219$ mm (48 in), $y_1 = 914$ mm (36 in), and $y_2 = 1829$ mm (72 in).

Data from sensors D9 and D10 were not used in computation of the numerical deflection function, so the deflection data measured at these locations were used to check the accuracy of the deflection function evaluated at each point. The coordinates of each of these two sensor locations were substituted in the deflection function for evaluation at each point; the resulting curves estimated using the deflection function were overlaid on the experimental data directly
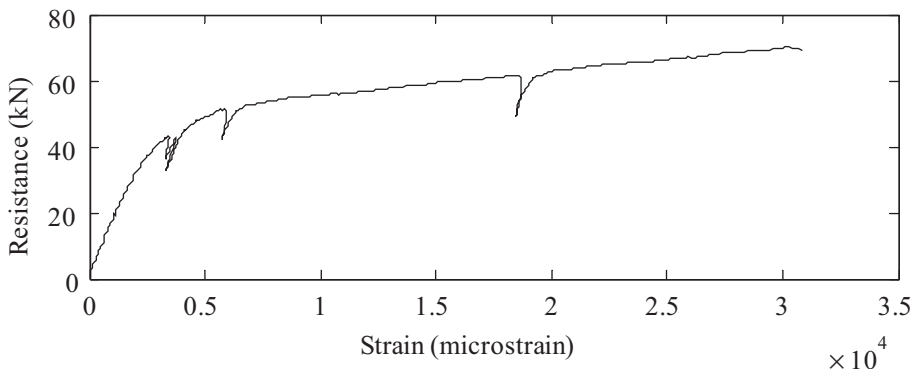

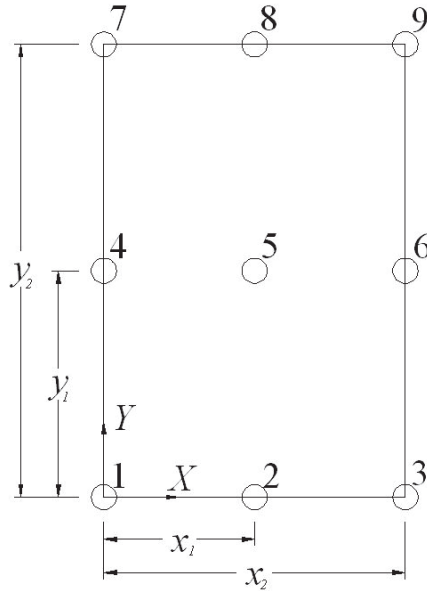Figure 6: Resultant force resistance versus SG2 strain (local resistance curve).

Figure 7: Diagram for Application of Interpolation Functions.

Table 3: Interpolation functions (N_i).

$$N_1 = \frac{(x-x_1)(x-x_2)(y-y_1)(y-y_2)}{(x_1)(x_2)(y_1)(y_2)} \quad N_2 = \frac{(x)(x-x_2)(y-y_1)(y-y_2)}{(x_1)(x_2-y_1)(y_1)(y_2)} \quad N_3 = \frac{(x-x_1)(x)(y-y_1)(y-y_2)}{(x_2-y_1)(x_2)(y_1)(y_2)}$$

$$N_4 = \frac{(x-x_1)(x-x_2)(y)(y-y_2)}{(x_1)(x_2)(y_1)(y_1-y_2)} \quad N_5 = \frac{(x)(x-x_2)(y)(y-y_2)}{(x_1)(x_1-x_2)(y_1)(y_1-y_2)} \quad N_6 = \frac{(x)(x-x_2)(y)(y-y_2)}{(x_2-x_1)(x_2)(y_1)(y_1-y_2)}$$

$$N_7 = \frac{(x-x_1)(x-x_2)(y-y_1)(y)}{(x_1)(x_2)(y_2-y_1)(y_2)} \quad N_8 = \frac{(x)(x-x_2)(y-y_1)(y)}{(x_1)(x_1-x_2)(y_2-y_1)(y_2)} \quad N_8 = \frac{(x-x_1)(x)(y-y_1)(y)}{(x_2-x_1)(x_2)(y_2-y_1)(y_2)}$$

measured at the corresponding locations (see Figs. 8 and 9). The maximum percent error for the maximum deflection estimated by the deflection function versus the experimental results was 11.9% with an average error of 6.2%. The maximum percent error of the absorbed energy (area under the resistance function) estimated by the deflection function versus that computed directly from experimental data was 12.6% with an average error of 6.7%.

For each curtain wall specimen the average deflection Δ_{ave} was computed by numerically taking a double integral of the deflection function over the area of a single quadrant and dividing by the area of the quadrant (2.23×10^6 mm^2 (3456 in^2)), thus

$$\Delta_{ave} = \frac{\iint \Delta(x,y)dA}{A} \tag{2}$$

The resultant force on a quadrant versus the average deflection of the quadrant can be presented as a global resistance curve (for specimen SPS-2) as shown in Fig. 10.
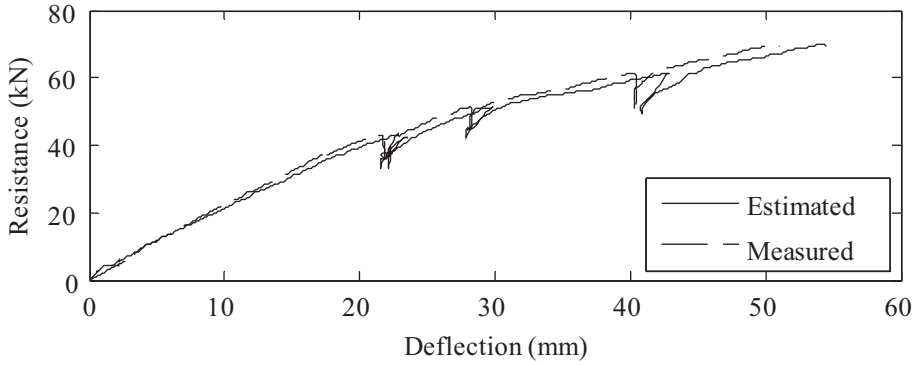
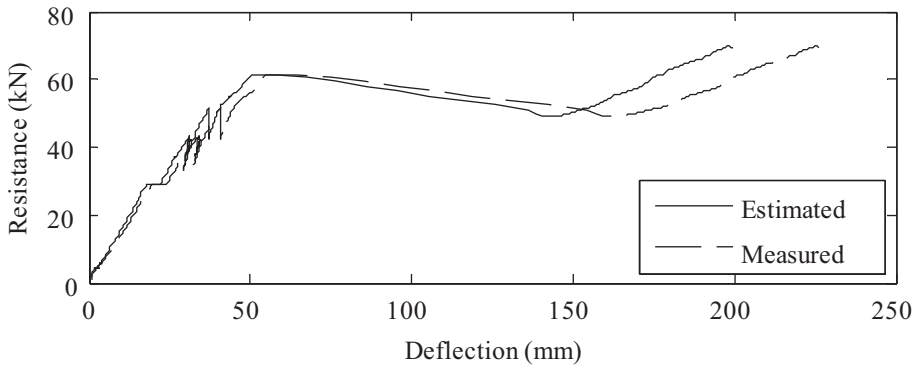Figure 8: Resistance curve comparison at location D9: estimated deflection versus measured deflection.

Figure 9: Resistance curve comparison at location D10: estimated deflection versus measured deflection.
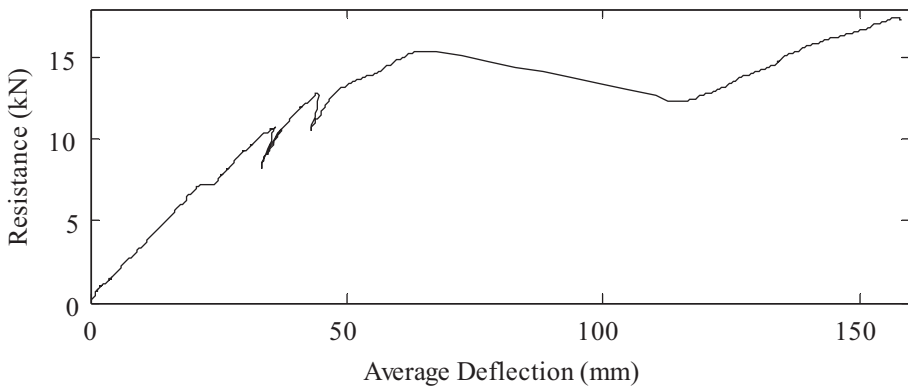

Figure 10: Resultant force resistance versus average deflection of a single curtain wall quadrant

3.2 Energy absorption capacity

Since the applied loading is equal to the curtain wall's resistance and the tests were conducted quasi-statically, the total energy absorbed by a quadrant of the curtain wall system up to ultimate failure (ultimate energy absorption capacity of a quadrant) is obtained by integrating the global resistance curve of Fig. 10. The result is shown in Fig. 11 as a function of the quadrant's average deflection.

If all lites failed at precisely the same time and had identical deflection patterns during testing, the ultimate energy absorption capacity of the entire curtain wall system would simply be four times that of a single quadrant. However, the absorbed energy computed from deflection measurements taken over a single quadrant (i.e. Lite 1 and its surrounding mullions) is dependent upon the sequence of lite cracking events and deflection patterns over *all* quadrants. Thus each quadrant, in general, had a different ultimate energy absorption capacity that could only be represented by the capacity measured over Lite 1. To address this limitation the available experimental data was used in conjunction with notes taken on the sequence of events during specimen testing, and the ultimate energy absorbed in Lites 2 through 4 was estimated from that absorbed in Lite 1. For the wet-glazed specimens a multiplier of 3.8, on average, was computed to estimate the ultimate energy absorption capacity of the entire curtain wall based on the absorbed energy measured in the single quadrant. For the dry-glazed specimen a multiplier of 2.4 was computed to estimate the ultimate energy absorption capacity of the entire curtain wall based on the absorbed energy measured in the single quadrant. This significantly smaller multiplier for the dry-glazed specimen is primarily due to the fact that only two glass lites underwent any membrane behavior (i.e. involving large deflections) prior to ultimate failure during the experiment. This indicates that one or both of these cracked lites would create a debris hazard (i.e. be ejected into the occupied building space) before the other two remaining lites would attain their membrane behavior.

The absorbed energies for each entire curtain wall specimen are given in Table 4 up to each of the three limit states: first cracking of glass, first yield of mullions, and ultimate failure (fracture/breach of the system). The ultimate energy absorbed by the wet-glazed specimens reached an average of 6.60 kJ (4.87 k-ft) while the ultimate energy absorbed by the dry-glazed specimen was only 2.06 kJ (1.52 k-ft).
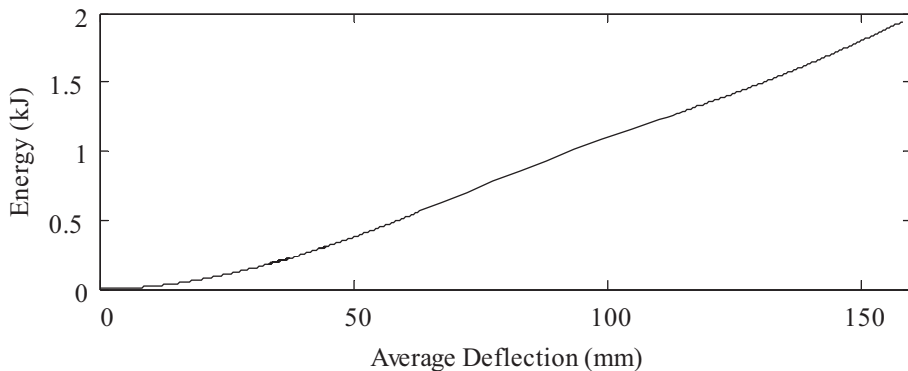

Figure 11: Energy absorbed by a single curtain wall quadrant versus average deflection.

Table 4: Absorbed energies for each entire curtain wall specimen.

Specimen	First Cracking*	First Yield**	Ultimate Failure	Failure Type
SPS-1	0.79 kJ	1.02 kJ	7.31 kJ	1
	(0.59 k-ft)	(0.75 k-ft)	(5.39 k-ft)	
SPS-2	0.36 kJ	1.92 kJ	7.16 kJ	3
	(0.27 k-ft)	(1.42 k-ft)	(5.28 k-ft)	
SPS-3	0.25 kJ	2.46 kJ	5.94 kJ	1
	(0.19 k-ft)	(1.82 k-ft)	(4.38 k-ft)	
SPS-4	0.44 kJ	2.13 kJ	5.98 kJ	3
	(0.33 k-ft)	(1.57 k-ft)	(4.41 k-ft)	
Average	0.46 kJ	1.88 kJ	6.60 kJ	-
	(0.34 k-ft)	(1.39 k-ft)	(4.87 k-ft)	
COV	0.50	0.33	0.11	-
SPG-1	0.53 kJ	1.74 kJ	2.06 kJ	3
	(0.39 k-ft)	(1.28 k-ft)	(1.52 k-ft)	

*First cracking of any glass lite. **First yield at SG2 of the center vertical mullion.

Table 5: Maximum mullion end rotations and mullion mid-height deflections.

Specimen	Maximum mullion end rotation	Mullion mid-height deflection
SPS-1	0.14 rad (7.9°)	144.8 mm (5.7 in)
SPS-2	0.15 rad (8.4°)	157.5 mm (6.2 in)
SPS-3	0.13 rad (7.2°)	132.1 mm (5.2 in)
SPS-4	0.12 rad (6.8°)	111.8 mm (4.4 in)
Average	0.13 rad (7.5°)	137.2 mm (5.4 in)
COV	0.10	0.1429
SPG-1	0.072 rad (4.1°)	68.6 mm (2.7 in)

It is noted for the wet-glazed specimens that the coefficient of variation (COV) quickly decreases as the limit states represent increasing damage levels (i.e. first cracking, first yield, and ultimate failure).

3.3 Maximum mullion end rotations

Maximum mullion end rotations were computed from measured and interpolated deflections along the center vertical mullion when the curtain wall reached ultimate failure; the maximum mullion end rotations include both elastic and plastic mullion behavior. Table 5 summarizes the maximum mullion end rotations and the corresponding mid-height mullion deflections for each test specimen. Wet-glazed specimens reached an average maximum mullion end rotation of 7.5°; the corresponding average mid-height deflection of the center vertical mullion was approximately L/25, where L is the clear span of the curtain wall's vertical mullions. The maximum mullion end rotation of the dry-glazed specimen was 4.1°; the corresponding mid-height mullion deflection was approximately L/50.

4 ANALYTICAL RESISTANCE FUNCTION

In order to simplify nonlinear dynamic analyses or design, it is common to approximate a complex load-deflection resistance curve with a linear elastic-perfectly plastic (bilinear) resistance function. For the wet-glazed curtain wall system with laminated glass lites, three quantities are required to define this function: the slope of the linear elastic region, the maximum elastic deflection (or resistance), and an ultimate deflection value (corresponding to ultimate failure of the system). For energy-based procedures it is important that the energy under the approximate resistance function be very nearly equal to the energy under the actual resistance curve.

Obtaining the exact solution for elastic deflections of a curtain wall system (as a function of applied load) is complex due to difficulties arising from representing support (boundary) conditions of its individual elements as well as from its global support conditions. Due to this complexity and the approximate nature of the analytical resistance function itself, it is justified and much simpler to model elastic deflections by 'adding' the deflections of the individual elements comprising the curtain wall system. Using small deflection theory for a simply supported plate, the deflections of the plate (glass lite) subjected to a uniform pressure are added to the bending deflections of the uniformly loaded beams (mullions) that support it along its vertical edges. The horizontal beams (mullions), however, are modeled as rigid links; they remain straight and their connections to the vertical mullions are pinned, thus they only effectively provide support for the short edges of the plate. According to Behr *et al.* [9] laminated glass lites at room temperature deflect approximately like monolithic glass lites of the same dimensions with a thickness equal only to the thickness of the glass (i.e. the thickness of the PVB interlayer is not included); thus the thickness of the glass plate was taken to be 9.525 mm (0.375 in) in all resistance function computations. The resulting elastic deflection solution as a function of applied pressure is approximated by

$$w(x,y) = \left(\frac{w_{mo}(y) - w_{mc}(y)}{a} \right) x + w_{mc}(y) + w_p(x,y) \tag{3}$$

where: $w_{mo}(y) = \dfrac{p\left(\dfrac{a}{2}\right)y}{(24 E_A I_{mo})(L^3 - 2Ly^2 + y^3)}$ is the deflection of the outer mullion,

$w_{mc}(y) = \dfrac{pay}{(24 E_A I_{mc})(L^3 - 2Ly^2 + y^3)}$ is the deflection of the center mullion,

$w_p(x,y) = \dfrac{4p}{\pi^6 D} \displaystyle\sum_m \sum_n \left[\dfrac{(1-(-1)^m)(1-(-1)^n)}{mn\left(\left(\dfrac{m}{a}\right)^2 + \left(\dfrac{n}{b}\right)^2\right)^2} \sin\left(\dfrac{m\pi x}{a}\right)\sin\left(\dfrac{n\pi y}{b}\right) \right]$ is the deflection

of a simply supported (glass) plate,

p is the applied pressure,

$D = \dfrac{E_G t^3}{12(1 - v^2)}$ is the flexural rigidity of the glass plate,

E_A is Young's modulus of aluminum (61.4 GPa (8.9×10^6 psi)),

E_G is Young's modulus of glass (71.7 GPa (10.4×10^6 psi)),

v is Poisson's ratio of glass (0.22),

I_{mo} is the moment of inertia of the outer mullion, including one glass flange of width $6t$, (2.764×10^6 mm^4 (6.64 in^4)),

I_{mc} is the moment of inertia of the center mullion, including two glass flanges, each of a width of $8t$, (2.914×10^6 mm^4 (7.00 in^4)),

t is the thickness of the glass plate, excluding the thickness of the PVB interlayer (9.525 mm (0.375 in),

a is the center to center spacing of the vertical mullions (1219 mm (48 in)),

b is the distance from the curtain wall support to the center horizontal mullion (1702 mm (67 in)), and

L is the clear span between supports (3404 mm (134 in)).

The origin of the coordinate system for eqn (3) is at the bottom bolted connection of the center vertical mullion, a small distance above the lower left corner of Lite 1 (see Fig. 1); thus plate bending in the small horizontal strip between the support and the lower edge of the glass lite is neglected in the deflection approximation. Equation (3) is valid over one quadrant of the curtain wall; that is: $0 \leq x \leq a$ and $0 \leq y \leq b$.

Equation (3) can be used to approximate the slope of the elastic portion of any 'local' load-deflection resistance function by plotting the deflection (on the abscissa) as a function of applied pressure on the ordinate. In computing the moments of inertia of the vertical mullions the contributions of the glass 'flanges' from the neighboring lites were included. This produced a more accurate slope for the elastic region of the resistance function than if the flanges were ignored. The tributary widths used to compute the equivalent uniform load for the vertical mullions are explicitly included in the expressions for w_{mo} and w_{mc}. Making use of eqn (3) and averaging the deflections as represented by eqn (2), the elastic stiffness for the global resultant force resistance function was found to be 1.26 kN/mm (7.17×10^3 lb/in); see the elastic region of the analytical curve in Fig. 12.
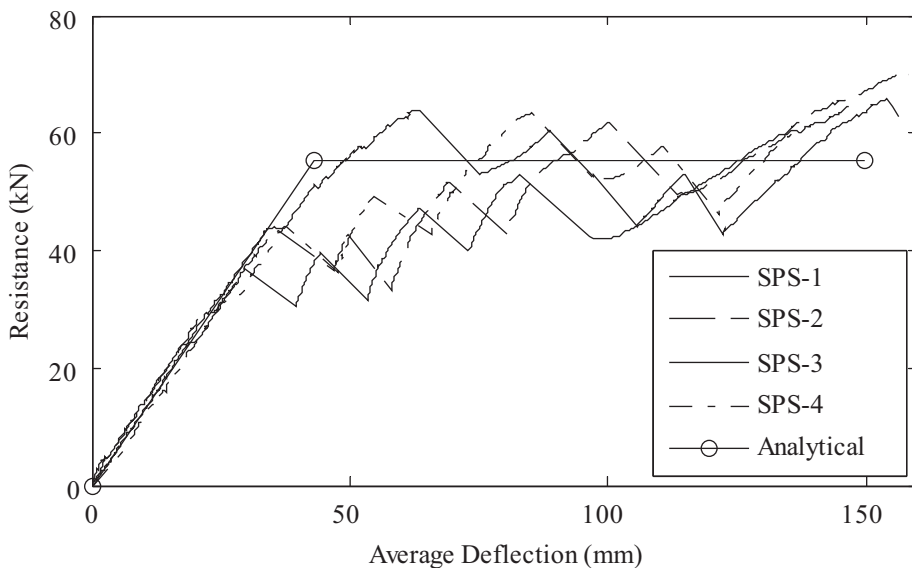

Figure 12: Comparison of experimental resistance curves to the analytical resistance function.

The maximum local elastic deflection at any point on the curtain wall can be calculated using eqn (3), limited by the applied pressure (or resultant force) that causes a plastic hinge to form at mid-height of the center vertical mullion. For the wet-glazed curtain walls studied in this program (curtain walls with reasonably sized elements), this is roughly the maximum capacity of the system until later in its response when it behaves globally like a membrane with the intrinsic large deflections. For curtain walls of different configurations and/or different relative element sizes, the designer/analyst must check to ensure that this state can be attained prior to ultimate failure of the system. Plastic hinge formation was calculated using the mullion's effective section properties. On average plastic hinge formation at mid-height of the center vertical mullion corresponded to an applied resultant force of 54.9 kN (1.235×10^4 lb); see the analytical curve in Fig. 12.

Finally the ultimate deflection of the local load-deflection resistance function must be determined; this is the deflection value that corresponds to the ultimate limit state (ultimate failure), where the curtain wall will no longer act as a protective barrier. This value is difficult, and perhaps impractical, to compute using fundamental mechanics equations. Therefore, in this paper the ultimate deflection is obtained from the average of the experimental results. The average maximum deflection at the mid-height of the center vertical mullion, 137.2 mm (5.4 in), is given in Table 5. As seen by comparing Figs. 4 and 5, maximum deflections at the center of a glass lite, 268.5 mm (10.57 in), were approximately twice the maximum mullion's deflection. After application of eqn (2), the maximum average deflection of the entire, global curtain wall was found to be 149.9 mm (5.9 in). Figure 12 is an overlay of the experimentally determined resistance curves and the analytically determined resistance function as a function of average deflection; all five plots in the figure are for the entire curtain wall (as opposed to just a single quadrant). The ultimate energy under the analytical resistance function is 7.05 kJ (5.2 k-ft), which is 6.8% higher than that under the average of the experimentally based resistance curves.

Guidance is not provided to compute the resistance function for a dry-glazed curtain wall with laminated glass lites because the wet-glazed system will perform better since it has an ultimate energy absorption capacity that is more than three times that of the dry-glazed system. The better performing wet-glazed system is recommended for resisting blast loads.

5 APPROXIMATE ENERGY-BASED EXPRESSION FOR SIMPLIFIED NONLINEAR BLAST DESIGN

Based on the conservation of energy applied to a nonlinear single degree of freedom (NSDOF) system, an approximate expression is presented for initial design (or simplified analyses) of a curtain wall system subjected to blast loading. When the fundamental (natural) period of a structural system is more than five times the dynamic load duration, the dynamic loading can be assumed, with reasonable accuracy, to be an impulse. Further, using the definition of impulse, for design purposes it is conservative to assume that the entire impulse i is converted to the initial velocity v of the NSDOF system, thus

$$v = \frac{i}{m} \tag{4}$$

The kinetic energy of the system is given by

$$KE = \frac{1}{2}mv^2 \tag{5}$$

and, after substitution of eqn (4) into eqn (5), the *initial* kinetic energy of the system can be written as

$$KE = {i^2}\big/{2m} \tag{6}$$

At the instant corresponding to the system's maximum deflection its velocity, and therefore its kinetic energy, is equal to zero. At this time all the system's initial kinetic energy has been transformed to energy internal to the system (i.e. the energy stored in its effective 'spring'); if the structure is at the threshold of ultimate failure, this internal energy equals the ultimate energy absorption capacity of the NSDOF system. Thus the conservation of energy gives

$$\frac{i^2}{2m} = \frac{R_m^2}{k\left(\mu - \dfrac{1}{2}\right)} \tag{7}$$

This equation, which conservatively ignores the loss of energy due to damping, was presented in Biggs [3]. Applying this expression to a blast resistant curtain wall system:

$i = K_L \times I$ is the effective reflected impulse of the blast load,

K_L is the effective load adjustment factor,

I is the actual reflected impulse,

$m = K_m \times M$ is the effective mass of the system,

K_M is the effective mass adjustment factor,

M is the mass of the entire curtain wall,

R_m is the maximum resistance of the curtain wall system,

k is the effective stiffness of the curtain wall system,

$\mu = \dfrac{y_m}{y_{el}}$ is the ductility of the curtain wall system,

y_m is the maximum deflection of the curtain wall system, and

y_{el} is the elastic deflection of the curtain wall system.

The right hand side of eqn (7) is simply the total area under the resistance function, the ultimate energy absorption capacity of the curtain wall system. Rearranging eqn (7), the expression that estimates the maximum impulse a curtain wall can resist while behaving as a protective barrier is

$$i_{max} = \frac{R_m \sqrt{2\mu - 1}}{\omega} \tag{8}$$

where $\omega = \sqrt{\dfrac{k}{m}}$ is the natural circular frequency of the curtain wall.

Rearranging eqn (7) with the experimental resistance curve in mind, a convenient equation for the maximum impulse a curtain wall can resist is

$$i_{max} = \sqrt{2m}\sqrt{\frac{R_m^2}{k\left(\mu - \dfrac{1}{2}\right)}} \tag{9}$$

Now the term under the second radical in eqn (9) is understood to be the total area under the experimental resistance curve up to ultimate failure.

Effective mass, effective stiffness, and effective load values for the simplified NSDOF system are commonly computed by multiplying the respective actual values of the real structure by adjustment factors. Following Biggs [3], the K_M factor is used for mass adjustment and the K_L factor is used for stiffness and applied loading adjustment. Generally, the values for each adjustment factor vary with the assumed shape function (deflection function) over the system's full range of response – from elastic to elastic-plastic and eventually to fully plastic deflections.

Over the full range of system response – elastic to fully plastic deflections – normalizing the assumed shape function by the *average* deflection will produce K_L factors that are always equal to unity. The analytical shape function used in this paper for the elastic range is given by eqn (3) and was normalized by the average deflection. K_M factors, however, vary over the range of system response. Using the numerical shape function [eqn (1) normalized by eqn (2)] obtained from experimental data, the K_M factor was found to be approximately equal to 1.1 in the elastic region and increased to 1.2 as the 'fully plastic' regime was approached. By contrast, a K_M factor of 1.2 was computed for the elastic range using the approximate analytical shape function given by eqn (3) and normalized by the average deflection. [A K_M factor was not computed beyond the elastic limit using an analytical shape function since only the elastic shape function given by eqn (3) was used in this work.] In light of these analyses, a constant K_M factor of 1.2 will be reasonably accurate over the entire range of system response.

6 BLAST RESISTANCE OF CONVENTIONAL AND NEARLY CONVENTIONAL CURTAIN WALLS

Three different curtain wall systems of identical configuration and support conditions (see Fig. 1) are compared to illustrate how incremental modifications to the conventional system can significantly improve blast resistance. System 1 is the (hypothetical) conventional system – dry-glazed monolithic glass lites – and is used only as the basis for comparisons. (The conventional system is not recommended for applications where blast loads may be of concern.) Systems 2 and 3 make incremental changes to System 1. System 2 (i.e. specimen SPG-1) uses dry-glazed *laminated* glass lites in place of the monolithic glass lites of System 1; System 3 (i.e. the SPS specimen series) *wet-glazes* laminated glass lites to the framing system. All three systems have an actual mass of 267 kg (1.53 lb-s^2/in), an effective mass of 320 kg (1.83 lb-s^2/in), and an actual (and effective) stiffness of 1.26 kN/mm (7.17×10^3 lb/in). As a result, all three systems have an analytically determined natural circular frequency of 62.7 rad/s. The experimentally determined (fundamental) natural circular frequency, computed from free vibration tests of the wet-glazed curtain wall with laminated glass lites, was 67.2 rad/s. The analytical value differs by only 6.7% when compared to the experimental value.

The second row of Table 6 lists the ultimate energy absorption capacity for each of the curtain wall systems. The values in columns 2–4 are computed from experimentally based resistance curves, and the value in column 5 is computed from the analytical resistance function for the wet-glazed system with laminated glass lites. The ultimate energy absorption capacity of System 1, the conventional system, is estimated from the area under the experimentally obtained resistance function up to the average occurrence of first cracking, beyond which the curtain wall becomes a debris hazard.

Substituting the effective mass into eqn (9) and using the ultimate energy absorption capacities given in the second row of Table 6, the ultimate impulses each curtain wall system could 'safely' resist are given in the third row of Table 6. Dividing Row 3 by the curtain wall's

Table 6: Blast resistance of different curtain wall systems.

System No.	1 (Exp.)	2 (Exp.)	3 (Exp.)	3 (Anal.)
Ult. Energy Abs. Cap.	0.48 kJ (0.35 k-ft)	2.06 kJ (1.52 k-ft)	6.60 kJ (4.87 k-ft)	7.05 kJ (5.20 k-ft)
Ult. Impulse	552 N-s (124.0 lb-s)	1149 N-s (258.4 lb-s)	2057 N-s (462.5 lb-s)	2126 N-s (477.9 lb-s)
Ult. Impulse	62 kPa-ms (9.0 psi-ms)	129 kPa-ms (18.7 psi-ms)	231 kPa-ms (33.5 psi-ms)	238 kPa-ms (34.5 psi-ms)

frontal area and changing units, Row 4 shows the ultimate impulse each curtain wall can safely resist in alternative units.

These comparisons demonstrate that System 2 would perform better than the conventional system (System 1), having the ability to safely withstand over twice the applied impulse. System 3 would safely withstand nearly four times the applied impulse as the conventional system (System 1). Using the analytical resistance function for System 3, the maximum impulse is 238 kPa-ms (34.5 psi-ms), which only differs by about 3% from the impulse computed using experimentally based resistance curves. Further, preliminary nonlinear dynamic FE blast simulations (using LS-Dyna) indicate that the estimated blast resistance of System 3 (columns 4 and 5 in Table 6) is conservative. Finally, the maximum impulses that can be safely resisted by each of these curtain wall systems can be easily related to explosive charge weights at given distances away from the face of the curtain wall (standoffs).

7 SUMMARY AND CONCLUSIONS

An experimental program was designed to investigate component and system behavior of nearly conventional curtain walls with a low level of blast resistance. System test results were presented by way of representative local load-deflection and load-strain resistance curves. Global load-deflection resistance curves were generated from local load-deflection resistance curves so that energy absorption capacities could be computed up to three limit states: first cracking, first yield, and ultimate failure. Maximum mullion end rotations and the corresponding mid-height mullion deflections were also presented to assist designers that routinely use SDOF (nonlinear) dynamic time-stepping algorithms.

A simplified procedure was presented to construct elastic perfectly plastic, global resistance functions that represent the behavior of the entire curtain wall system. This procedure is intended to facilitate blast resistant design for curtain walls of similar materials, configurations, and proportioning to the system investigated in this paper. As a system deviates from the one presented here, the designer is cautioned that the details of this construction procedure will lose their applicability. As a result, quasi-static destructive tests of the new system or a more involved mechanics-based procedure for constructing curtain wall resistance functions that explicitly considers the possibility and sequence of glass cracking, plastic hinging, tearing of the structural silicone sealant, and connection failure will be required. The latter might involve nonlinear FE simulations to extend the applicability of the simplified resistance function construction. In any event, once a global resistance function is adequately constructed, the simplified nonlinear design equation adapted in this paper can be used to estimate the blast resistance of the curtain wall in an impulse-dominated regime. If the

curtain wall's shape function (often assumed) is normalized by the average deflection, the value for K_L will always be unity, but a value for K_M must in general be computed for each shape function over each range of system response.

Using the ultimate energy absorption capacities computed from the experimentally determined resistance curves and the effective mass of the system, the blast resistance of three slightly different curtain wall systems was illustrated. A conventional system with the addition only of laminated glass (System 2) performed significantly better than the fully conventional system (System 1); it had over four times the ultimate energy absorption capacity, which resulted in the capacity to safely resist over twice the blast-induced impulse of the conventional system. Further improvement of System 2 was accomplished by wet glazing the laminated glass lites to supporting mullions with structural silicone sealant, producing System 3; System 3 had nearly 14 times the ultimate energy absorption capacity and nearly four times the blast resistance of the conventional system. It is observed that a four-fold increase in a curtain wall's ultimate energy absorption capacity is required for a doubling of its blast resistance; this is easily seen in the presented equations. For the wet-glazed system with laminated glass, the analytical resistance function led to an ultimate energy absorption capacity and a blast resistance that was, respectively, 6.8% and 3.0% higher than that computed from the experimentally based resistance curves. Finally, preliminary nonlinear dynamic FE blast simulations using LS-Dyna indicate that the estimated blast resistance of System 3 [using eqns. (3) and (9)] is conservative.

Wet-glazed specimens attained an average maximum mullion end rotation of 7.5°, a value that agrees better with the suggestion of Dawson and Smilowitz [27] than the current design practice of limiting maximum mullion end rotations to 2°. The dry-glazed specimen only attained a maximum mullion end rotation of 4.1°, but this value is still significantly larger than the current design practice.

Increasing system 'ductility' while reducing the debris hazard are the primary requirements for enhancing the blast performance of curtain walls. For the curtain walls explored in this program, conventional extrusions, mullion-to-mullion connections, and connections to the structural back-up are adequate for low level blast resistance. Increased ductility was shown to rely on two important modifications relative to the conventional system: 1) the use of laminated glass lites that are 2) structurally glazed with structural silicone sealant. Structurally glazing laminated glass lites allows cracked lites to behave like membranes, effectively transferring in-plane tensile stresses to the supporting framing system while behaving as a protective barrier.

The ultimate energy absorption capacity and the maximum mullion end rotations could be somewhat larger than the values presented in this paper if more damage to the curtain wall system were to be tolerated by the designer. Even after mullion fracture (ultimate failure) the overall wet-glazed curtain wall system continued to resist additional applied load. Thus the failure definition adopted here may be deemed conservative and a different failure definition could be used to achieve slightly more economical blast resistant designs. Additional conservatism arises here since material dynamic increase factors (from high stain rates), damping mechanisms, the outboard monolithic lite of the IG unit, and the reduction of reflected blast pressures (impulses) due to the flexibility of the curtain wall system were not considered in this work.

The conservatism of the approximate design expression and the accuracy of FE simulations should be assessed by blast testing the resulting curtain wall specimens in an open-arena. These tests may also assist in the determination of appropriate material dynamic increase factors and more representative applied pressures which consider the flexibility of the curtain wall system.

ACKNOWLEDGEMENTS

REFERENCES

[1] Weggel, D.C. & Zapata, B.J., Laminated glass curtain walls and laminated glass lites subjected to low-level blast loading. *Journal of Structural Engineering*, **134(3)**, pp. 466–477, 2008. doi: http://dx.doi.org/10.1061/(ASCE)0733-9445(2008)134:3(466)

[2] Weggel, D.C., Zapata, B.J. & Kiefer, M.J., Properties and dynamic behavior of glass curtain walls with split screw spline mullions. *Journal of Structural Engineering*, **133(10)**, pp. 1415–1425, 2007. doi: http://dx.doi.org/10.1061/(ASCE)0733-9445(2007) 133:10(1415)

[3] Biggs, J.M., *Introduction to Structural Dynamics*, McGraw-Hill, Inc., 1964.

[4] Beason, W.L. & Morgan, J.R., Glass failure prediction model. *Journal of Structural Engineering*, **110(2)**, pp. 197–222, 1984. doi: http://dx.doi.org/10.1061/(ASCE)0733-9445(1984)110:2(197)

[5] Vallabhan, C.V.G., Interactive analysis of nonlinear glass plates. *Journal of Structural Engineering*, **102(2)**, pp. 489–502, 1983. doi: http://dx.doi.org/10.1061/(ASCE)0733-9445(1983)109:2(489)

[6] ASTM, *Standard Practice for Determining Load Resistance of Glass in Buildings*, *E1300-09a*, West Conshohocken, PA, 2009.

[7] Behr, R.A., Kremer, P.A., Dharani, L.R., Ji, F.S. & Kaiser, N.D., Dynamic strains in architectural glass subjected to low velocity impacts from small projectiles. *Journal of Materials Science*, **34**, pp. 5749–5756, 1999. doi: http://dx.doi.org/10.1023/A:1004702100357

[8] Behr, R.A., Minor, J.E. & Linden, M.P., Load duration and interlayer thickness effect on laminated glass. *Journal of Structural Engineering*, **112(6)**, pp. 1441–1453, 1986. doi: http://dx.doi.org/10.1061/(ASCE)0733-9445(1986)112:6(1441)

[9] Behr, R.A., Minor, J.E. & Norville, H.S., Structural behavior of architectural laminated glass. *Journal of Structural Engineering*, **119(1)**, pp. 202–223, 1993. doi: http://dx.doi.org/10.1061/(ASCE)0733-9445(1993)119:1(202)

[10] Makovicka, D. & Lexa, P., Dynamic response of window glass plates under explosion overpressure. *Proc., 2nd Int. Conf. on Struct. Under Shock and Impact II*, Computational Mechanics Publications: Southampton, England, pp. 380–392, 1992.

[11] Norville, H.S., King, K.W. & Swofford, J.L., Behavior and strength of laminated glass. *Journal of Engineering Mechanics*, **124(1)**, pp. 46–53, 1998. doi: http://dx.doi.org/10.1061/(ASCE)0733-9399(1998)124:1(46)

[12] Vallabhan, C.V.G., Asik, M.Z. & Kandil, K., Analysis of structural glazing systems. *Computers & Structures*, **65(2)**, pp. 231–239, 1997. doi: http://dx.doi.org/10.1016/S0045-7949(96)00284-2

[13] Norville, H.S. & Conrath, E.J., Blast-resistant glazing design. *Journal of Architectural Engineering*, **12(3)**, pp. 129–136, 2006. doi: http://dx.doi.org/10.1061/(ASCE)1076-0431(2006)12:3(129)

[14] ASTM, *Specifying an Equivalent 3-Second Duration Design Loading for Blast Resistant Glazing Fabricated with Laminated Glass*, *F2248-09*, West Conshohocken, PA, 2003.

[15] AAMA, *Structural Performance: Poured and Debridged Framing Systems*, American Architectural Manufacturers Association: Palatine, IL, 1990.

[16] Goodno, B.J., Glass curtain wall elements: properties and behavior. *Journal of. Structural Division*, **105(6)**, pp. 1121–1136, 1979.

[17] Hautekeer, J.P., Monga, F., Giesecke, A. & O'Brien, B., The use of silicone sealents in protective glazing applications. *Glass processing days*, Tampere, Finland, pp. 298–302, 2001.

[18] Vallabhan, C.V.G., Chou, G.D. & Minor, J.E., Seal forces in structural glazing systems. *Journal of Structural Engineering*, **116(4)**, pp. 1080–1089, 1990. doi: http://dx.doi.org/10.1061/(ASCE)0733-9445(1990)116:4(1080)

[19] Zarghamee, M.S., Schwartz, T.A. & Gladstone, M., Seismic behavior of structural silicone glazing. *ASTM Special Tech. Publ*., **(1286)**, pp. 46–59, 1996.

[20] Behr, R.A., Belarbi, A. & Culp, J.H., Dynamic racking tests of curtain wall in-plane and out-of-plane motions. *Earthquake Engineering Structural Dynamics*, **24(1)**, pp. 1–14, 1995. doi: http://dx.doi.org/10.1002/eqe.4290240102

[21] Memari, A.M., Behr, R.A. & Kremer, P.A., Dynamic racking crescendo tests on architectural glass fitted with anchored pet film. *Journal of Architectural Engineering*, **10(1)**, pp. 5–14, 2004. doi: http://dx.doi.org/10.1061/(ASCE)1076-0431(2004)10:1(5)

[22] Memari, A.M., Chen, X., Kremer, P.A. & Behr, R.A., Seismic performance of two-side structural silicone glazing systems. *Journal of ASTM International*, **3(10)**, pp. 1–10, 2006.

[23] Pantelides, C.P. & Behr, R.A., Dynamic in-plane racking tests of curtain wall glass elements. *Earthquake Engineering Structural Dynamics*, **23(2)**, pp. 211–228, 1994. doi: http://dx.doi.org/10.1002/eqe.4290230208

[24] Craig, J.I. & Goodno, B.J., Response measurements for glass cladding panels. *Journal of Structural Division*, **107(11)**, pp. 2199–2214, 1981.

[25] Goodno, B.J. & Craig, J.I., Response studies of glass cladding panels. *Proc., Int. Symp. on Bhvr. of Bldg. Sys. and Bldg. Comp.*, Nashville, TN, pp. 137–158, 1979.

[26] Clift, C.D., Curtain wall designs for wind and blast: three case studies. *Journal of Architectural Engineering*, **12(3)**, pp. 150–155, 2006. doi: http://dx.doi.org/10.1061/(ASCE)1076-0431(2006)12:3(150)

[27] Dawson, H. & Smilowitz, R., Inelastic dynamic response of curtainwall systems to blast loading. *Journal of ASTM International*, **4(5)**, pp. 1–5, 2007.

[28] U.S. General Services Administration, *GSA Test Protocol GSA-TS01-2003 US General Services Administration Standard Test Method for Glazing and Window Systems Subject to Dynamic Overpressure Loadings*, US General Services Administration: Washington, D.C., 2003.

[29] ARA, *WINGARD-MP (Multi-Pane Edition) User Guide*, Applied Research Associates, 2010.

[30] Cussen, R. & Van Eepoel, P., Inelastic dynamic finite-element design of glazed façade systems for blast loading. *Crossing Borders: Structures Congress 2008*, Vancouver, Canada, pp. 1–11, 2008.

[31] Edel, M.T. & Kumar, D., Blast design approach comparisons for curtain wall. *Proc., 2010 Struct. Cong.*, Orlando, FL, pp. 2076–2089, 2010. doi: http://dx.doi.org/10.1061/41130(369)188

[32] ASTM, *Standard Test Methods for Tension Testing Wrought and Cast Aluminum- and Magnesium-Alloy Products*, B557-06, West Conshohocken, PA, 2006.

[33] Norville, H.S. & Conrath, E.J., Considerations for blast-resistant glazing design. *Journal of Architectural Engineering*, **7(3)**, pp. 80–86, 2001. doi: http://dx.doi.org/10.1061/(ASCE)1076-0431(2001)7:3(80)